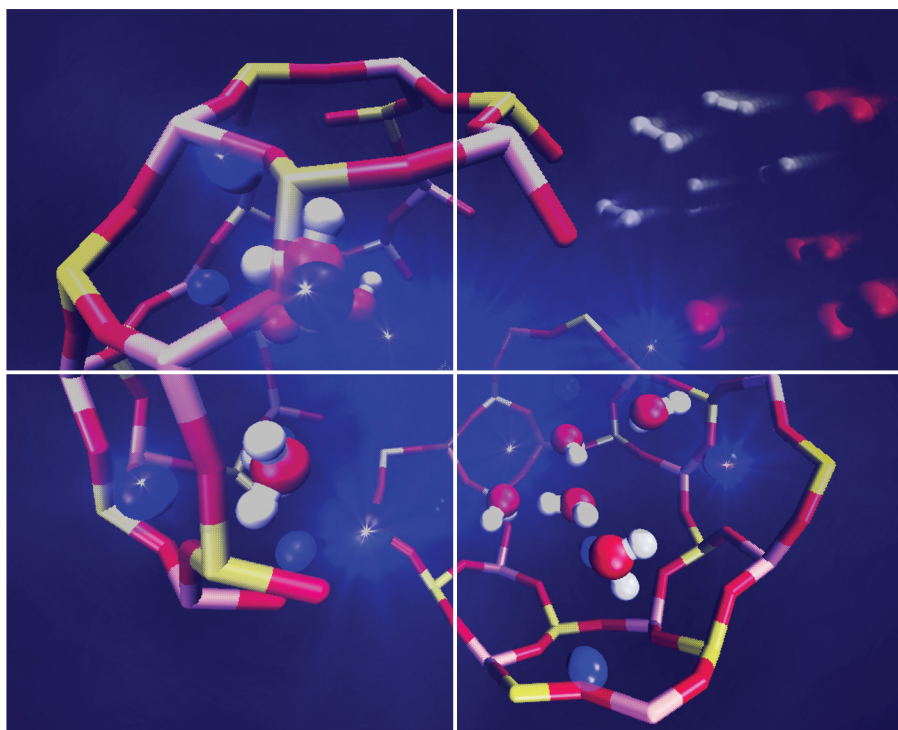


Volume 10 | Number 2 | 21 January 2023

**10**  
YEARS  
ANNIVERSARY



# INORGANIC CHEMISTRY

## FRONTIERS



CHINESE  
CHEMICAL  
SOCIETY



ROYAL SOCIETY  
OF CHEMISTRY

[rsc.li/frontiers-inorganic](https://rsc.li/frontiers-inorganic)

Cite this: *Inorg. Chem. Front.*, 2023, **10**, 383

# Effect of the water coverage on the interaction of O<sub>2</sub> and H<sub>2</sub> with the Na-LTA zeolite by first-principles simulations

Joharimanitra Randrianandraina,<sup>a</sup> Michael Badawi,<sup>b</sup> Christophe Ramseyer,<sup>a</sup> Bruno Cardey,<sup>a</sup> Jean-Emmanuel Groetz,<sup>a</sup> Noah Perreau,<sup>a</sup> Freddy Torrealba-Anzola,<sup>a</sup> Caroline Chambelland,<sup>c</sup> Didier Ducret<sup>c</sup> and Manuel Grivet<sup>\*a</sup>

The very wide applications of LTA zeolites, e.g. tritiated water storage, imply that a precise atomic-scale description of the adsorption processes taking place in their structure is crucial. The zeolite structure seems to have a catalytic effect on the O<sub>2</sub>/H<sub>2</sub> recombination during the storage process after water radiolysis. To look closely at the conditions that could bring O<sub>2</sub> and H<sub>2</sub> to this particular point, we have conducted investigations using static DFT and systematic *ab initio* molecular dynamics calculations. We have investigated the interaction of these two molecules with the sodium cations, on which the adsorption capacity of the Na-LTA zeolite depends. The O<sub>2</sub> and H<sub>2</sub> molecules' behaviour inside the cavities is linked to the Na<sup>+</sup> position and availability. The latter is regulated by the presence of H<sub>2</sub>O which interacts with Na<sup>+</sup> in a stronger way than O<sub>2</sub> and H<sub>2</sub>. Thus, the adsorption studies of different mixtures (O<sub>2</sub>/H<sub>2</sub>O, H<sub>2</sub>/H<sub>2</sub>O and H<sub>2</sub>/O<sub>2</sub>) have been carried out to characterise the competition between water and other guest molecules. The absence of an obvious interaction between the adsorbates strongly suggests a potential reaction path involving the catalytic effect of the zeolite. Since we have been able to show that the behaviour of O<sub>2</sub> and H<sub>2</sub> molecules is directly affected by the water coverage rate, the reaction path is very likely to be affected too. These results mark a step towards the description of a recombination mechanism between O<sub>2</sub> and H<sub>2</sub> in a zeolite structure, a crucial issue for such systems involving tritiated water adsorbed in nanoporous materials.

Received 16th June 2022,  
Accepted 2nd November 2022

DOI: 10.1039/d2qi01280d

rsc.li/frontiers-inorganic

## 1. Introduction

With the development of projects requiring the use of tritium such as ITER, the treatment of tritiated waste will be a major environmental issue in the future. This waste can be found in the form of tritiated water adsorbed in nanoporous materials such as zeolites, during which a water radiolysis phenomenon occurs where oxygen and hydrogen are the main gas products. Experimental studies carried out by L. Frances *et al.*<sup>1,2</sup> showed a progressive decrease of these products from the resulting gaseous formation through time until their total disappearance. Although the water radiolysis reaction is enhanced by the catalytic effect of the zeolite into which it is contained,

L. Frances *et al.* presumed that the aluminosilicate structure also contributes to the recombination of O<sub>2</sub> and H<sub>2</sub> back to H<sub>2</sub>O, with which is associated the gaseous quantity decrease. The period in which these decays occur depends on the loading rate of water present in the zeolite: the higher the loading rate, the later they start. The strong affinity between the water molecules and the Na<sup>+</sup> cations of the Na-LTA zeolite, as observed in our previous study,<sup>3</sup> leads us to link this time lag to the hindrance to the access of O<sub>2</sub> and H<sub>2</sub> molecules to the cationic sites by H<sub>2</sub>O. Therefore, the zeolite contributes to the catalysis of the recombination reaction of the two molecules through the Na<sup>+</sup> cations. This implies that the dihydrogen and dioxygen molecules must interact with the zeolite, *i.e.*, the cations, for the recombination reaction to start.

The role of the adsorbent surface as a catalyst has already been studied on other surfaces than zeolites, mostly metallic.<sup>4–8</sup> G. J. K. Acres<sup>9</sup> observed the inhibitory effect (as a decrease of the reaction rate) of water on H<sub>2</sub>/O<sub>2</sub> recombination on a platinum surface. As the surface catalyses the dissociation of dihydrogen and dioxygen molecules, its coating by water prevents both from interacting with the surface. Acres thus

<sup>a</sup>Laboratoire Chrono-Environnement, UMR 6249, Université de Bourgogne Franche-Comté, F-25000, Besançon, France. E-mail: manuel.grivet@univ-fcomte.fr; Tel: +33 3 81 66 65 16

<sup>b</sup>Laboratoire de Physique et Chimie Théoriques, UMR 7019, CNRS, Université de Lorraine, F-54000 Nancy, France. E-mail: michael.badawi@univ-lorraine.fr; Tel: +33 3 72 74 98 67

<sup>c</sup>CEA, Centre d'études de Valduc, F-21120 Is-sur-Tille, France



showed the necessity for the molecules to be in contact with the adsorbing surface in order to be activated, in good agreement with the observations from the experimental works by L. Frances *et al.*<sup>1</sup> concerning the delaying effect of water on the decrease of the amounts of O<sub>2</sub> and H<sub>2</sub> molecules in zeolites. L. Morales,<sup>10</sup> who studied the recombination on a plutonium dioxide surface, emphasizes the important role of a catalyst that the surface plays in the reaction and minimizes that of the radicals formed during radiolysis. Lloyd and Eller<sup>11</sup> define this catalytic role of the surface as being a platform on which the O<sub>2</sub> and H<sub>2</sub> molecules dissociate before recombining. Like Acres,<sup>9</sup> Morales also noted that the presence of water on the surface reduces the rate of the reaction because its strong affinity limits the access of O<sub>2</sub> to the surface. The adsorption studies of H<sub>2</sub>O, O<sub>2</sub> and H<sub>2</sub> in zeolites showed that the order of the adsorption affinity of the molecules in zeolites is as follows: H<sub>2</sub>O ≫ O<sub>2</sub> > H<sub>2</sub><sup>12–18</sup> as represented in Fig. 1. The affinity of O<sub>2</sub> for zeolites is thus more important than that of H<sub>2</sub>. In addition to the presence of H<sub>2</sub>O, this difference also affects the rate of the reaction between O<sub>2</sub> and H<sub>2</sub> as shown by G. J. K. Acres,<sup>9</sup> who observed a faster rate of reaction when O<sub>2</sub> is previously present on the Pt surface and inversely when it is the case of H<sub>2</sub>. A strong interaction of the molecule, whether O<sub>2</sub> or H<sub>2</sub>, with the surface thus accelerates its activation to dissociation followed by recombination. Numerous studies of O<sub>2</sub> and H<sub>2</sub> molecules' dissociation in zeolites<sup>19–21</sup> highlighted the contribution of cations on their activation. These play a significant part in the catalysis by zeolites, especially by controlling the interaction between adsorbates and adsorbents. These observations lead us to assume that a possible path to recombination between the two adsorbed molecules is through their dissociation *via* the adsorbent surface, where water plays a disruptive role.

To our knowledge, no study has yet been carried out to describe the O<sub>2</sub>/H<sub>2</sub> competition, let alone their recombination

mechanism in zeolites with Na<sup>+</sup> cations, neither numerically nor experimentally. Yet, the different works cited above show the interest of understanding such competition governed by H<sub>2</sub>O in an accessible and no less efficient porous material such as a zeolite. Given the stronger interaction of O<sub>2</sub> molecules with zeolites compared to that of H<sub>2</sub>, we have described the O<sub>2</sub>...Na<sup>+</sup> and H<sub>2</sub>...Na<sup>+</sup> interactions and looked carefully at the influence of the occupancy rate of Na<sup>+</sup> sites by H<sub>2</sub>O since there is probably a competition between the stable products of radiolysis and the water molecules. The recombination mechanism of the two molecules will not be described in this paper since our study on this topic is still in progress, but we will focus here on the path that leads to this phenomenon through the O<sub>2</sub> and H<sub>2</sub> molecules' adsorption on dehydrated and hydrated Na-LTA zeolites. In particular, we demonstrate the important role played by the Na<sup>+</sup> cation in the activation of O<sub>2</sub> and H<sub>2</sub> and assess how the water loading rate in the zeolite affects its catalytic efficiency. For this purpose, numerical methods like static and dynamic DFT have been used to provide a detailed description of the behavior of these molecules on the adsorption sites of the studied zeolites.

## 2. Materials and methods

### 2.1. Z4A and ZK4 models

Two zeolites from the LTA framework have been used for this work. Since the Z4A unit cell (672 atoms) cannot be reduced due to Lowenstein's rule,<sup>22,23</sup> the smaller elementary lattice of the ZK4 zeolite was used as a substitute for *ab initio* molecular dynamics (AIMD) calculations.

The optimised unit cell of the dehydrated Z4A framework has the chemical formula Na<sub>96</sub>Si<sub>96</sub>Al<sub>96</sub>O<sub>384</sub><sup>24</sup> with a Si/Al ratio of 1 and the following lattice parameters:  $a = 24.47 \text{ \AA}$ ,  $b = 24.65 \text{ \AA}$ ,  $c = 24.82 \text{ \AA}$ ,  $\alpha = 90.7^\circ$ ,  $\beta = 89.8^\circ$  and  $\gamma = 90.1^\circ$ . These are very similar to the initial values given by J. J. Pluth *et al.*<sup>25</sup> The ZK4 unit cell was created from the optimised Z4A by extracting 1/8<sup>th</sup> of its lattice, *i.e.*, one sodalite cage. Si and Al distributions have been rearranged to avoid the Al–O–Al sequence according to the model used by Yoshida *et al.*,<sup>26</sup> who already used the ZK4 structure to substitute the Z4A unit cell for AIMD calculations. The ZK4 unit cell has the formula Na<sub>9</sub>Si<sub>15</sub>Al<sub>9</sub>O<sub>48</sub> with a Si/Al ratio of 1.66 and the lattice parameters  $a = 12.35 \text{ \AA}$ ,  $b = 12.28 \text{ \AA}$ ,  $c = 12.19 \text{ \AA}$ ,  $\alpha = 90.3^\circ$ ,  $\beta = 90.4^\circ$ , and  $\gamma = 89.7^\circ$  after DFT geometry optimisation.

Both Z4A and ZK4 structures have three types of windows (4R, 8R and 8R) that allow the communication between the different cavities (Fig. 2). The 4R window is a pathway allowing access from the  $\alpha$  and  $\beta$  cages to a rectangular prism. The 6R window is a passage between the  $\alpha$  and  $\beta$  cages and the 8R window gives access between two  $\alpha$  cages.

The Na<sup>+</sup> cations are located on three cationic sites, denoted I, II and III, respectively (Fig. 3). In the Z4A unit cell, they are distributed as follows: 64 Na<sup>+</sup> on site I on the 6R windows, denoted Na(I), 24 on site II inside the 8R windows, denoted Na(II), and 8 on site III, in front of the 4R windows, denoted

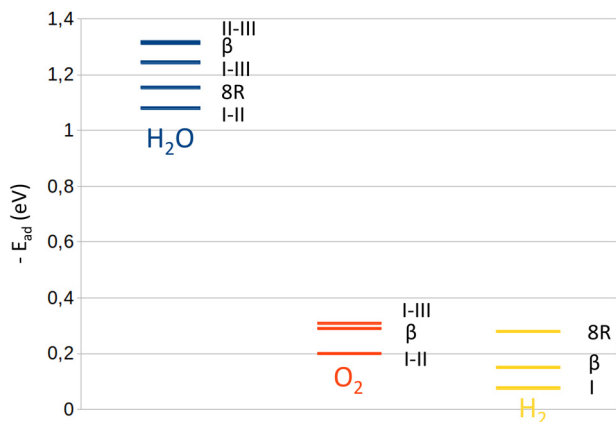


**Fig. 1** Adsorption energy level calculated from our simulations for each molecule, H<sub>2</sub>O (blue), O<sub>2</sub> (red) and H<sub>2</sub> (yellow), inside the Na-LTA zeolite according to the adsorption site where they are located: between two cationic sites (II–III, I–III, and I–II), on the 8R window (8R), and inside the  $\beta$  cage or near Na(i) (I).



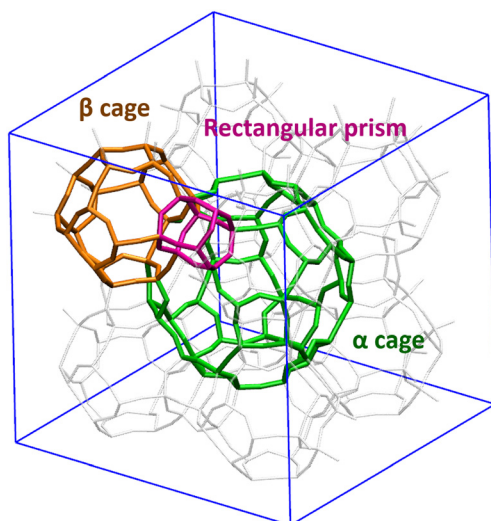


**Fig. 2** Different cavities constituting a unit cell of the LTA type zeolite – the  $\alpha$  cage (green) is the largest one, surrounded by the  $\beta$  cages (orange), connected to each other through the rectangular prisms (purple).

Na(III). Thus, all 6R and 8R windows are occupied by one cation, in agreement with the description made by J. J. Pluth *et al.*<sup>25</sup> To ensure the presence of local atomic configurations that can be found in both ZK4 and Z4A structures, the Na<sup>+</sup> cations inside the ZK4 unit cell were distributed as follows: 6 on site I, 2 on site II and 1 on site III (Fig. 3).

## 2.2. Computational methods

To perform geometry optimisation and energy determination, density functional theory calculations were carried out using the Vienna *Ab initio* Simulation Package (VASP 5.4) code<sup>27</sup> with the generalized gradient approximation and the Perdew–Burke–Ernzerhof exchange correlation functional.<sup>28,29</sup> Pseudopotentials were described by using the projector-augmented wave method,<sup>30,31</sup> and the D2 dispersion correction of Grimme<sup>32,33</sup> was applied for the description of van der Waals forces. The plane wave cut-off energy was set to 520 eV. The Brillouin zone and the reciprocal space were sampled through the  $\Gamma$ -point sampling. The convergence criterion for ionic relaxation was set to 0.01 eV  $\text{\AA}^{-1}$  for static DFT calculations.

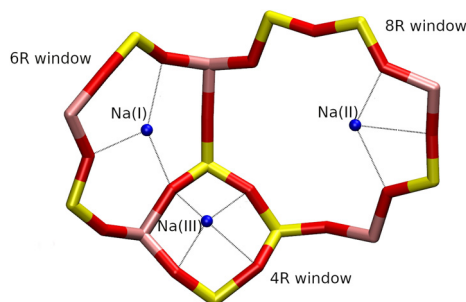


**Fig. 3** Cationic sites (blue) of the Na-LTA structures.

*Ab initio* molecular dynamics simulations (AIMD) were performed with the electronic parameters set for static DFT relaxations over a minimum total simulation time of 110 ps including a 15 ps of equilibration period. Systems containing hydrogen atoms require the use of a time step smaller than 1 fs (ref. 34 and 35) to avoid fictitious molecular splitting. Another method, that we did not apply in this work, consists of increasing the mass of the hydrogen atom to 3, which corresponds to the atomic mass of tritium. Thus, the time step of 1 fs would be suitable for reaction studies.<sup>36,37</sup> The energy criterion for electronic convergence was set to  $10^{-4}$  eV. The temperature was set to a mean of 298 K using the Andersen thermostat.<sup>38</sup> The adsorption energies for static simulations (or binding energies, depending on the community) were calculated using the following expression:

$$E_{\text{ads}} = \frac{E_{\text{system}} - N_{\text{W}} \times E_{\text{W}} - E_{\text{Z}}}{N_{\text{W}}} \quad (1)$$

where  $E_{\text{system}}$  is the total energy of the system,  $E_{\text{W}}$  is the mean energy of H<sub>2</sub>O molecules,  $E_{\text{Z}}$  is the total energy without H<sub>2</sub>O molecules, and  $N_{\text{W}}$  is the number of H<sub>2</sub>O molecules.

All of the illustration figures of the system and the RDF graphs have been generated with the VMD (visual molecular dynamics) program.<sup>†</sup><sup>39</sup>

Because of the large size of the system with the Z4A unit cell (672 atoms), several optimisation steps were taken to ensure a smooth and accurate energy minimization of the structure. A first classical geometry optimisation was necessary using the general utility lattice program<sup>40</sup> in order to preoptimise the structure, thus saving the computation time for the following DFT calculations as performed in our previous study.<sup>3</sup>

## 3. Results and discussion

### 3.1. O<sub>2</sub> adsorption

To clarify how the O<sub>2</sub> molecule interacts with the zeolite, we studied its adsorption in three types of structures (Fig. 4): purely silicated (Pur-Si), with one Al and one Na (1Al–1Na), and with two Al and two Na (2Al–2Na). Table 1 summarizes the calculated adsorption energies for these three systems.

These results show the important effect of Na<sup>+</sup> cations on the adsorption of the O<sub>2</sub> molecule inside the zeolite. It is the most stable when the molecule is interacting with two cations where the adsorption energies are ~158% and ~38% stronger than those for the silicated and 1Al–1Na systems, respectively.

The cationic sites of the LTA zeolite are distributed in its  $\alpha$  and  $\beta$  cages. Although the probability for the O<sub>2</sub> molecule to be present in the  $\beta$  cage is very weak, as shown in experimental adsorption studies, inside the dehydrated zeolites,<sup>16</sup> water radiolysis leading to the production of oxygen occurs in both cavities. In this context, the  $\beta$  cage can therefore be occupied

<sup>†</sup> <https://www.ks.uiuc.edu/Research/vmd/>.



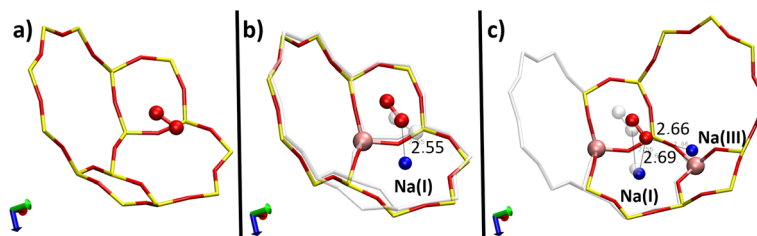


**Fig. 4** Optimised positions of O<sub>2</sub> in the  $\alpha$  cage of three different structures: purely silicated without the Na<sup>+</sup> cation (a), with one Na<sup>+</sup> cation (b) and two Na<sup>+</sup> cations (c) – the position of the O<sub>2</sub> molecule before the addition of a supplementary cation is represented in transparent, interatomic distances are given in Å.

**Table 1** Calculated adsorption energy ( $E_{ad}$ ) of the O<sub>2</sub> molecule on each of these three structures: without the Na<sup>+</sup> cation (Pur-Si), with one Al atom and one Na<sup>+</sup> cation (1Al-1Na), and with two Al atoms and two Na<sup>+</sup> cations (2Al-2Na)

System	$E_{ad}$ (eV)	O <sub>2</sub> ...Na(Å)	O–O (Å)
Pur-Si	–0.114	—	1.23
1Al-1Na	–0.213	2.55	1.23
2Al-2Na	–0.294	2.66 and 2.69	1.23

by the O<sub>2</sub> molecule and the  $\alpha$  cage. Thus, we have studied its adsorption inside both these parts of the Na-LTA zeolites.

Inside the  $\beta$  cage, the optimised position of the O<sub>2</sub> molecule lies unsurprisingly between two Na<sup>+</sup> cations, with an adsorption energy of –0.290 eV. This stability is justified by the distribution of the electronic density around the oxygen atoms of O<sub>2</sub> obtained from an electron localization function (ELF) study, as shown in Fig. 5, which illustrates the optimised position of the molecule inside the  $\beta$  cage. The electrons are distributed around the oxygen atoms of the molecule on a perpendicular plane to the O–O axis, which limits the configuration possibilities of the molecule with respect to the cation. In this represented configuration, each oxygen atom of O<sub>2</sub> is interacting with one Na<sup>+</sup> cation, with O(O<sub>2</sub>)...Na<sup>+</sup> distances of 2.68 and 2.75 Å and a O–O bond length of 1.24 Å.

The dynamics (AIMD) calculations show that another possible configuration of O<sub>2</sub> inside the  $\beta$  cage is when only one of

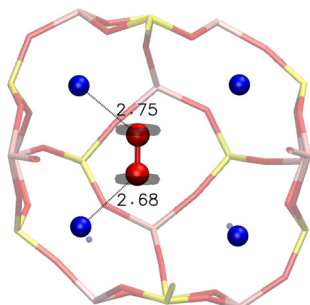


**Fig. 5** Optimised position of the O<sub>2</sub> molecule inside the  $\beta$  cage after static DFT calculations – the calculated electron localisation function (ELF), around O(O<sub>2</sub>) atoms, is represented with an isovalue of 0.78, interatomic distances are given in Å.

its two O atoms interacts with two Na<sup>+</sup> cations, as shown in Fig. 7 (config. 1). The mobility of the O<sub>2</sub> molecule inside the  $\beta$  cage is then mainly oscillating between its four surrounding Na<sup>+</sup> cations by alternating these configurations and gives the adsorbed molecule a very strong stability on its adsorption site.

A comparison between both the configurations will be discussed in the adsorption studies inside the  $\alpha$  cage part, where both of them can be encountered as well.

Since the interaction of the O<sub>2</sub> molecule with the zeolite framework is mainly through the Na<sup>+</sup> cation, its location inside the  $\alpha$  cage should follow the distribution of the cationic sites (I, II and III). The radial function distribution (RDF) calculation of the Na...Na distance (Fig. 6) indicates that the shortest distance is located around 4 Å (first peak), mainly associated with those between Na(I) and Na(III) (~3.90 Å) but also between Na(I) and Na(II) (~4.4 Å), while the majority of Na<sup>+</sup> cations are separated from each other by around 4.8 Å (second peak), which is associated with the distance between Na(I) cations. The shortest distance between the Na(II) and Na(III) cations is located around ~5.2 Å. Therefore, taking into account the O<sub>2</sub>...Na distances calculated previously (2.6–2.7 Å), it is highly likely for the O<sub>2</sub> molecule to be located between two cations. Hence, we have chosen the initial positions of the molecule before optimisation using static DFT calculations with reference to this observation.

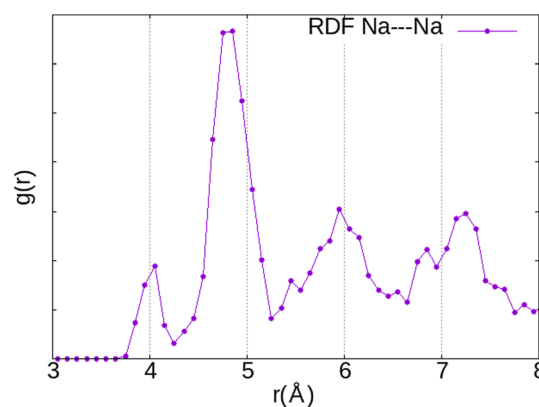


**Fig. 6** Radial distribution function (RDF) of the distances between the Na<sup>+</sup> cations.



The mobility of the cations of the Na-LTA zeolite depends on the sites on which they are located. The cations of sites II and III are more mobile than those located on site I.<sup>41–44</sup> This is due to the coordination of Na<sup>+</sup> with the oxygen atoms of the window where the site is located. This mobility of the cations has an influence on the stability of the adsorbed molecules, in particular, that of O<sub>2</sub>. For the static studies inside the  $\alpha$  cage, we placed the O<sub>2</sub> molecule on the two cationic sites of the Na-LTA zeolite between two cations: Na(I)–Na(II) and Na(I)–Na(III). For each position, the two configurations described above have been applied (Fig. 7):

- config. 1: one oxygen atom interacting with two cations,
- config. 2: each of the oxygen atoms of the molecule interacting with a cation.

The calculation of the adsorption energies shows that the affinity of the adsorbed O<sub>2</sub> molecule with the zeolite structure varies according to its stabilized position. This affinity seems stronger when the guest molecule is located between Na(I) and Na(III), and preferably positioned according to the configuration config. 2 (Table 2). This can be explained by the higher mobility of the Na(III) cation compared with those belonging to the other sites.<sup>25,41,45</sup> The Na<sup>+</sup> cation and the O<sub>2</sub> molecule thus approach each other mutually. Moreover, the O–O bond seems to stretch in this particular position (1.25 Å).

Whether or not this elongation (+0.02 Å compared with the bond length in the gaseous phase) is significant enough to be considered as a preparation of the molecule for dissociation remains to be discussed. When O<sub>2</sub> is located between Na(I) and Na(II), its bond length is shortened by 0.01 Å from config. 1 to config. 2 (Table 2). However, this configuration seems to be more favorable energetically speaking and referring to the relationship between the bond order and the bond length made by T. Chen and T. A. Manz,<sup>46,47</sup> a variation of the bond length means a variation of the bond order. In our case, we observe a decrease of the O–O bond order, *i.e.* a weakening of the bond.

From a dynamics perspective, both configurations can be encountered during the evolution of the O<sub>2</sub> molecule in the  $\alpha$  cage (Fig. 8). In a time interval of 120 ps, the molecule has moved from its initial cationic site to a neighbouring site with a residence time of about 30 ps at each site, whereas the molecule remains 1 to 2 ps in one configuration before changing to another.

Therefore, the cations slow down the diffusion of the O<sub>2</sub> molecule inside the  $\alpha$  cage by moving it from one cationic site to another – at least in the case of a fully dehydrated zeolite where all Na<sup>+</sup> sites are available to the molecule.

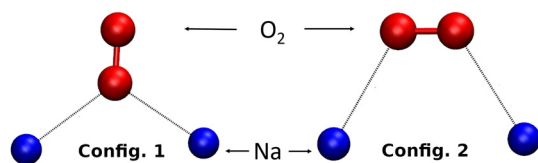


Fig. 7 Possible configurations of the O<sub>2</sub> molecule when interacting with two Na<sup>+</sup> cations.

Table 2 Comparison, after static DFT calculations, between the two configurations (config. 1 and config. 2) of the O<sub>2</sub> molecule positioned between two Na<sup>+</sup> cations located on sites I and II (Na(I)/Na(II)) and on sites I and III (Na(I)/Na(III)) in the  $\alpha$  cage – the adsorption energy ( $E_{ad}$ ) is expressed in eV and the other values are distances expressed in Å where: Na(X)⋯Na(Y) is the distance between two cations, O(O<sub>2</sub>)⋯Na(X) is the distance between the oxygen atom of the molecule and one Na<sup>+</sup> cation, (X and Y = I, II or III), and diff is the difference between the calculated values in config. 1 and config. 2

Position	Values	Config. 1	Config. 2	Diff
Inside the $\beta$ cage	$E_{ad}$	—	−0.290	—
	Na(I)⋯Na(II)	—	4.47	—
	O(O <sub>2</sub> )⋯Na(I)	—	2.68 and 2.75	—
	O <sub>2</sub> bond length	—	1.24	—
Na(I)/Na(II)	$E_{ad}$	−0.200	−0.233	0.033
	Na(I)⋯Na(II)	4.38	4.45	0.07
	O(O <sub>2</sub> )⋯Na(I)	2.90	2.68	0.22
	O(O <sub>2</sub> )⋯Na(II)	2.75	2.63	0.12
	O <sub>2</sub> bond length	1.24	1.23	0.01
Na(I)/Na(III)	$E_{ad}$	−0.309	−0.332	0.023
	Na(I)⋯Na(III)	3.85	3.92	0.07
	O(O <sub>2</sub> )⋯Na(I)	2.65	2.63	0.02
	O(O <sub>2</sub> )⋯Na(III)	2.57	2.50	0.07
	O <sub>2</sub> bond length	1.24	1.25	0.01

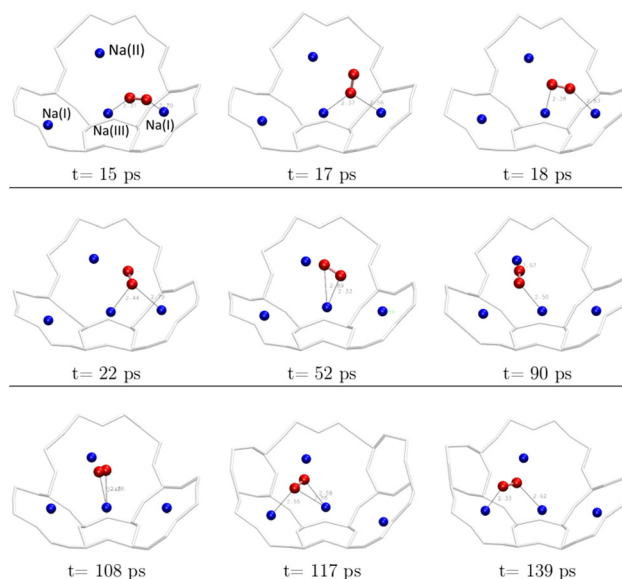


Fig. 8 Transition from one cationic site to another of the O<sub>2</sub> molecule during the AIMD calculations (duration: 139 ps) – each figure represents a snapshot of the position of the molecule at moment *t*.

Actually, given the stronger interaction of water with the Na<sup>+</sup> cation compared with that of O<sub>2</sub>,<sup>16,18,48,49</sup> the latter has only access to the cationic sites that are still unoccupied by the H<sub>2</sub>O molecules. Indeed, static DFT calculations of the co-adsorption of the two molecules have shown that the presence of O<sub>2</sub> near the H<sub>2</sub>O adsorption site is not sufficient to remove the water molecule from it, either in the  $\beta$  or  $\alpha$  cage.



**3.1.1. O<sub>2</sub>/H<sub>2</sub>O mixture studies.** To perform the adsorption of O<sub>2</sub> in the hydrated zeolite, O<sub>2</sub> was introduced near the H<sub>2</sub>O molecule, whose position was previously optimised. The studies were performed in the vicinity of four H<sub>2</sub>O adsorption sites located in our previous work (Fig. 9) where the H<sub>2</sub>O molecule is: (a) inside the  $\beta$  cage, (b) on the 8R window, considered as a very stable site in the  $\alpha$  cage, (c) between two cations Na(I) and Na(III) and (d) between two cations Na(II) and Na(III).

The first observation is that, in most configurations, the water molecule remains on its adsorption site (Fig. 9a–c) where its equilibrium position has already been well optimised. Even the fact that both O<sub>2</sub> and H<sub>2</sub>O molecules interact with the same Na(III) cation (Fig. 9c) is not sufficient to release the water molecule from its adsorption site. Instead, it reorients itself while remaining in interaction with the two cations Na(I) and Na(III). However, when the H<sub>2</sub>O molecule is placed between Na(II) and Na(III) (Fig. 9d), the water molecule is only in a pseudostable position considering the distance of Na(II)⋯Na(III) (~5.2 Å), which is longer than those of Na(I)⋯Na(III) and Na(I)⋯Na(II) as we have seen earlier on the description of the intercationic distances (Fig. 6). The perturbation brought by the addition of the O<sub>2</sub> molecule naturally leads the water molecule to reconfigure its equilibrium position for a more stable site nearby, *i.e.*, the 8R window. One of the atoms of O<sub>2</sub> is then interacting with two cations Na(II) and Na(III), which are separated by a Na(II)⋯Na(III) distance of 4.79 Å, with Na⋯O<sub>2</sub> distances of 2.60 and 2.52 Å, respectively, while the other oxygen atom is interacting with one Na(I) at a distance of 2.71 Å. The observations made on these systems do not show a clear interaction between H<sub>2</sub>O and O<sub>2</sub>, both molecules tend to favor interactions with the Na<sup>+</sup> cations. There is thus a competition between O<sub>2</sub> and H<sub>2</sub>O molecules to occupy the cationic sites. More precisely, since both molecules interact preferably with the Na<sup>+</sup> cations, the occupation of the site by the O<sub>2</sub> molecule depends on its availability, and thus its occupancy rate by H<sub>2</sub>O molecules. This was confirmed by our AIMD calculations where the evolution of two O<sub>2</sub> molecules inside the  $\alpha$  cage has been studied as a function of the number of water molecules in the cage ( $N$ ). As  $N$  increases, the dioxygen molecules have

less and less access to the cationic sites, as shown by the radial distribution function of the O<sub>2</sub>⋯Na distance (Fig. 10) where the intensity of the first peak (located at ~2.75 Å), representing the distance between O<sub>2</sub> and the nearest Na<sup>+</sup> cation, decreases as the water loading increases until  $N = 15$ . Then its intensity becomes lower than that of the other peaks located at other distances.

This correlates with the experimental observation by Izumi and Suzuki<sup>50</sup> where a clear decrease of the O<sub>2</sub> adsorption capacity of the Na-LTA zeolite is noted from a water loading rate of 15% (approximately ~15 H<sub>2</sub>O in the  $\alpha$  cage), which supports the role of Na<sup>+</sup> cations in the adsorption of the O<sub>2</sub> molecule. At this particular point of the water filling of the  $\alpha$  cage, it is relevant to state that the majority of the cations are occupied at least by one water molecule.<sup>3</sup> Accordingly, the interaction of the O<sub>2</sub> molecules with the cationic sites is more and more restricted by the presence of water until there is no (or very little) access to cations, as shown in Fig. 10 at  $N = 20$ , corresponding to the number of H<sub>2</sub>O molecules in the  $\alpha$  cage near the saturation of the zeolite which is around 25 H<sub>2</sub>O per  $\alpha$  cage.<sup>41,49,51,52</sup> At this stage of water filling, the O<sub>2</sub> molecules are mostly distributed around 6 Å from the nearest Na<sup>+</sup> cation, the majority peak is shifted by +3.25 Å with respect to the positions of the other water quantities, even if the O<sub>2</sub> molecules occasionally interact with the cations at a distance of 2.75 Å (Fig. 10,  $N = 20$ ). However, an increase in the number of water molecules does not promote the formation of hydrogen bonds between O<sub>2</sub> and H<sub>2</sub>O molecules, which remain mostly at a distance of 3.75 Å from each other, as shown by the radial distribution function of the distance O(O<sub>2</sub>)⋯H<sub>W</sub> between the oxygen atom of O<sub>2</sub> and the hydrogen atom of H<sub>2</sub>O (Fig. 11). Again, at  $N = 10$ , the reciprocal behavior of O<sub>2</sub> and H<sub>2</sub>O is different from those associated with other water quantities. The results obtained from Fig. 10 and 11 allow us to say that the mobility of the O<sub>2</sub> molecule in the  $\alpha$  cage is particularly

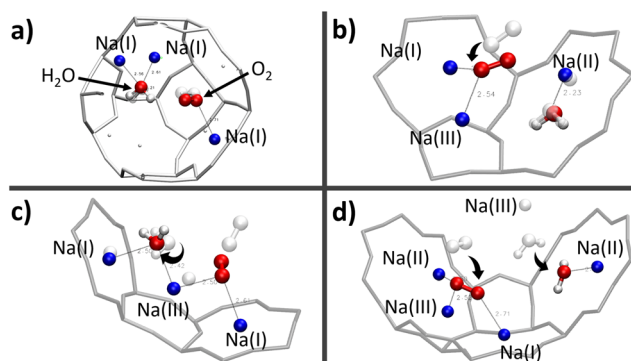


**Fig. 9** Optimised positions of the O<sub>2</sub>/H<sub>2</sub>O mixture for different configurations inside the  $\beta$  (a) and  $\alpha$  (b, c, and d) cages – the positions of the adsorbates before the optimisation are represented in transparent.

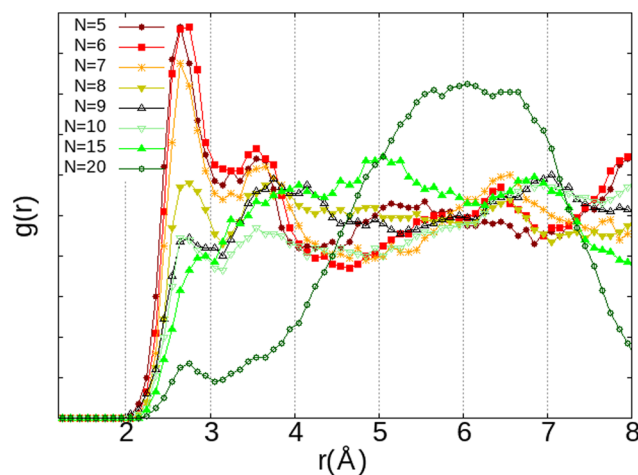


**Fig. 10** RDF of the O<sub>2</sub>⋯Na<sup>+</sup> distance depending on the number of H<sub>2</sub>O molecules ( $N$ ) inside the  $\alpha$  cage from AIMD calculations – each system is constituted of  $N$  H<sub>2</sub>O and 2 O<sub>2</sub>.



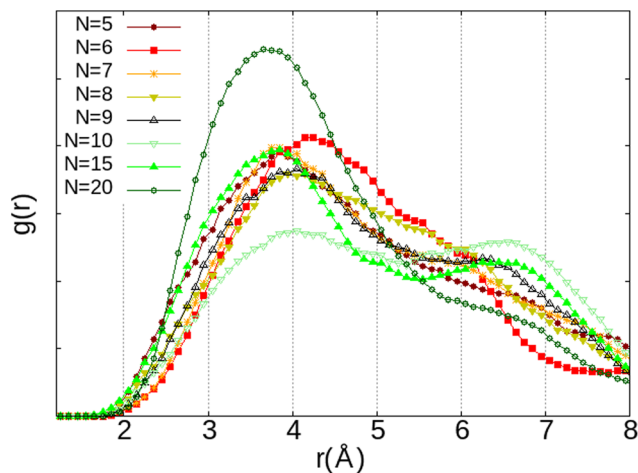


**Fig. 11** RDF of the distance between the oxygen atom of  $O_2$  and the hydrogen atom of  $H_2O$  ( $O_2 \cdots H_W$ ) as a function of the number of  $H_2O$  molecules ( $N$ ) inside the  $\alpha$  cage obtained from AIMD calculations.

important when 15 water molecules are present since as we said previously, all the cations are occupied by at least one  $H_2O$  molecule. This step represents the saturation of the cationic sites of the  $\alpha$  cage and the accentuation of the growth in the number of hydrogen bonds between the water molecules<sup>53</sup> (Fig. 12).

Therefore, the amount of water in the cavity not only affects the interaction of the  $O_2$  molecules with the zeolite but also their mobility. On the one hand because of the competition between the two molecules ( $O_2$  and  $H_2O$ ) for the occupation of the cationic sites, on the other hand because of the congestion created by the water molecules forming rings between them *via* hydrogen bonds and  $Na^+$  cations. One of the direct consequences of this phenomenon was observed experimentally by L Frances *et al.*<sup>1</sup> on the consumption of the gaseous phase composed, among other elements, of  $O_2$  that has been released

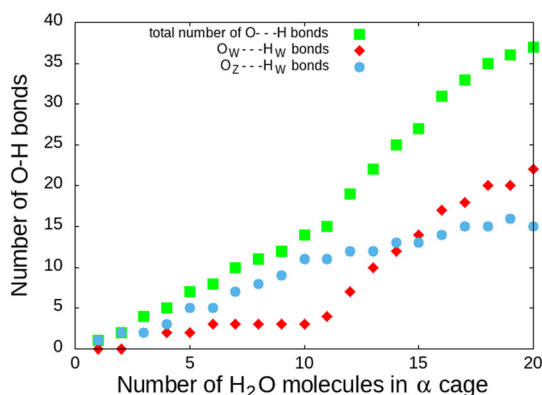


**Fig. 12** Number of H bonds during water filling of the  $\alpha$  cage of the Na-LTA zeolite –  $O_W \cdots H_W$  is the H-bond formed between the water molecules and  $O_Z \cdots H_W$  is the H-bond formed between the water molecule and the zeolite structure.<sup>53</sup>  $O \cdots H$  distances less than 2.1 Å have been taken into account as the H bond.

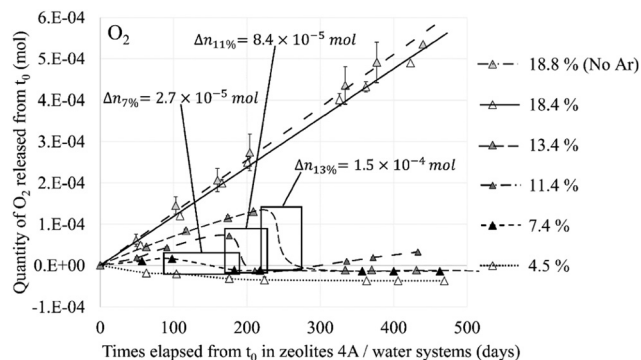


**Fig. 13** Released quantity of  $O_2$  from the NaA zeolite at different water loading rates – framed periods indicate the gas decrease and the quantity of reacting  $O_2$ . Reprinted with permission from L. Frances *et al.*<sup>1</sup> Copyright 2015 American Chemical Society.

following the radiolysis of water in the Na-A zeolite (Fig. 13). The delay between each decrease in the  $O_2$  component is closely related to the amount of water present in the structure, *i.e.*, the water loading rate that is indicated in mass % in the results. It is interesting to note that this decay does not occur when the zeolite is saturated, *i.e.*, when the  $O_2$  molecules in the zeolite do not have access to the  $Na^+$  sites because of their total occupation by water molecules. One of the hypothesis to explain this decrease in the quantity of  $O_2$  is its recombination with  $H_2$ , which is also a product of water radiolysis, to form back water. This implies that the recombination reaction requires the contact of the reactants  $O_2$  and most likely  $H_2$  with the cations, which underlines the catalytic role of the zeolite.

Hence, as for the  $O_2$  molecule, we have studied the interaction of  $H_2$  with the Na-LTA zeolite and the other adsorbates ( $H_2O$  and  $O_2$ ).

### 3.2. $H_2$ adsorption

First, to describe the interaction of the  $H_2$  molecule with the zeolite framework, its adsorption was studied through the static DFT method inside two types of LTA structures: purely silicated (no cation) and with one  $Na^+$  cation (Fig. 14).

The adsorption energy calculations yielded a more stable configuration when the molecule is adsorbed on a cation at the  $H_2 \cdots Na$  distances of 2.34 and 2.41 Å (Table 3). When adsorbed inside the structure composed of one  $Na^+$  cation, the distance of 2.64 Å between the  $H_2$  molecule and one oxygen atom of the zeolite framework indicates the formation of a weak hydrogen bond between the adsorbate and the adsorbent. Therefore, the  $H_2$  molecule also interacts with the oxygen of the zeolite in addition to  $Na^+$ , although the latter remains the main actor in the interaction of  $H_2$  with the zeolite. The most stable configuration for the molecule seems to be when its two hydrogen atoms are in interaction with the same  $Na^+$  cation, which is described as the most stable equilibrium geometry for the  $Na^+H_2$  complex.<sup>54–56</sup>

The way  $H_2$  interacts with the oxygen atoms of the zeolite depends on its environment and the proximity of the oxygen



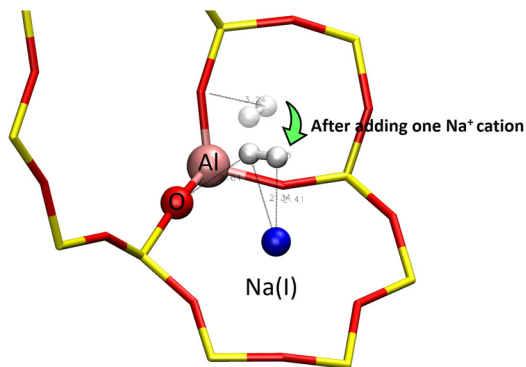


**Fig. 14** Optimised positions of the H<sub>2</sub> molecule (white) in the  $\alpha$  cage of two LTA structures: with and without the Na<sup>+</sup> cation – the position of the molecule before the addition of the Na<sup>+</sup> cation is represented in transparent.

**Table 3** Calculated adsorption energy ( $E_{ad}$ ) of the H<sub>2</sub> molecule in each of the two structures: without the Na<sup>+</sup> cation (Pur-Si) and with one Na<sup>+</sup> cation and one Al atom (1Al-1Na)

System	$E_{ad}$ (eV)	H <sub>2</sub> ...Na <sup>+</sup> (Å)	H <sub>2</sub> ...O <sub>Z</sub> (Å)	H-H (Å)
Pur-Si	-0.049	—	3.24	0.75
1Al-1Na	-0.182	2.34 and 2.41	2.64	0.75

atoms. For example, inside the  $\beta$  cage, the proximity between the oxygen atoms of the wall provided by the confinement of the cage gives H<sub>2</sub> the possibility to interact with two oxygen atoms from the zeolite wall, which results in an asymmetry in the distribution of the electronic isodensity around the molecule (Fig. 15) and an adsorption energy of -0.077 eV.

Elsewhere, inside the  $\alpha$  cage, H<sub>2</sub> adopts the same configuration as in the  $\beta$  cage, *i.e.*, the two hydrogen atoms are interacting with the same Na<sup>+</sup> cation, while a hydrogen bond is formed between the adsorbate and the adsorbent, with an adsorption energy of -0.151 eV. These interactions between the H<sub>2</sub> molecule and the zeolite remain short-range, the molecule very weakly perceives the effect of the adsorbent surface when it is placed close to the middle of the  $\alpha$  cage, ~4.5 Å from the nearest Na<sup>+</sup> cation (adsorption energy of -0.027 eV). It is interesting to note that this value represents a weaker

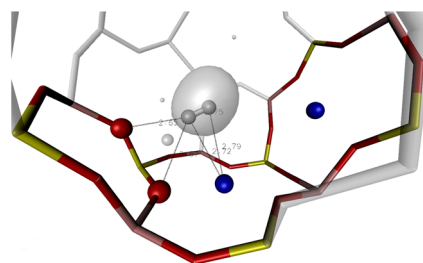


**Fig. 15** Optimised position of the H<sub>2</sub> molecule (white) in the  $\beta$  cage by two oxygen atoms (red) and one Na<sup>+</sup> cation (blue) – the calculated electron localisation function is represented at an isovalue of 0.986.

**Table 4** Calculated adsorption energy ( $E_{ads}$ ) of the H<sub>2</sub> molecule in the  $\alpha$  cage

Location	$E_{ad}$ (eV)	H <sub>2</sub> ...Na (Å)	H <sub>2</sub> ...O <sub>Z</sub> (Å)
Inside $\beta$	-0.077	2.72 and 2.79	2.65 and 2.67
Close to the $\alpha$ center	-0.027	4.57	5.38
Near the Na <sup>+</sup> cation in the $\alpha$ cage	-0.151	2.43 and 2.37	2.59

adsorption of the H<sub>2</sub> molecule compared to that in the purely silicated structure (-0.049 eV, Table 3). This can be explained by the position of the molecule which is closer to the walls of the zeolite in this latter case, the influence of the adsorbing surface through its oxygen atoms is therefore more important with respect to the case where the H<sub>2</sub> molecule is at least at 4.75 Å from the closest Na<sup>+</sup> cation and 5.38 Å from the nearest oxygen atom of the cage (Table 4). The values in Table 4 are given to compare the interactions of the H<sub>2</sub> molecule with the zeolite according to its localisation and configuration inside the  $\alpha$  cage. In each case, the bond length of the molecule remained equal to 0.75 Å. The adsorption of the H<sub>2</sub> molecule does not seem to affect its geometry, except for one particular configuration where it is located on a 8R window (Fig. 16).

When adsorbed on the 8R window, the two hydrogen atoms of the H<sub>2</sub> molecule interact with the same Na(II) cation at H<sub>2</sub>...Na<sup>+</sup> distances of 2.31 and 2.36 Å, each of them also form hydrogen bonds with the oxygen atoms of the window where the shortest H<sub>2</sub>...O<sub>Z</sub> distances are at 2.84 and 2.56 Å. This configuration gives the H<sub>2</sub> molecule a bond length of 0.76 Å (0.01 Å longer than for the other configurations). However, the most peculiar value is that of the adsorption energy of -0.280 eV, which is unusually strong for the H<sub>2</sub> molecule, because this implies a stronger adsorption than for some O<sub>2</sub> sites as seen in Fig. 1.

This “abnormally” high value of the adsorption energy of the H<sub>2</sub> molecule is also noticed by Areán *et al.*<sup>57</sup> for the same configuration, in their adsorption studies of the molecule in a CaA zeolite (of the LTA structure with Ca<sup>2+</sup> cations). They attribute this strong stability of the molecule to its particularly

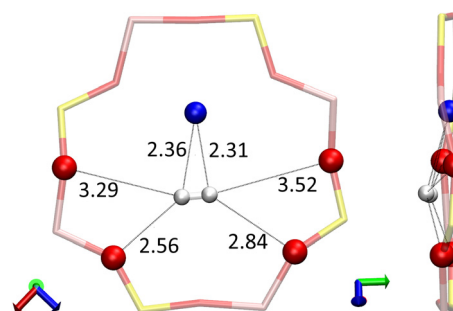


**Fig. 16** Particular configuration of the H<sub>2</sub> molecule (white) on the 8R window – in addition to the Na(II) cation (blue), each hydrogen atom of the molecule interacts with two oxygen atoms of the window, respectively, interatomic distances are given in Å.



favorable configuration with a strong electrostatic interaction with the oxygen atoms of the zeolite, in addition to its interaction with the cation. This configuration thus seems very stable for H<sub>2</sub>. It turns out that the 8R window is also among the most stable adsorption site for the H<sub>2</sub>O molecule inside the  $\alpha$  cage.<sup>3</sup> Further investigations are obviously needed on this particular adsorption site since it amplifies the catalytic effect of the zeolite on H<sub>2</sub>O and H<sub>2</sub> molecules. *Ab initio* molecular dynamics calculations inside the  $\alpha$  cage have confirmed the H<sub>2</sub> molecule preference to interact with the Na<sup>+</sup> cation instead of the oxygen atom of the zeolite, as shown by the radial distribution functions where the distances between the H<sub>2</sub> molecule and the Na<sup>+</sup> cations (H<sub>2</sub>...Na<sup>+</sup>) are mostly distributed around 2.45 Å (Fig. 17a). This result is consistent with the potential energy studies of the Na<sup>+</sup>-H<sub>2</sub> interaction,<sup>54,58</sup> albeit longer (~+0.1 Å) than the value that we have obtained from static calculations. The distribution for those between the adsorbed molecule and the oxygen atoms of the structure (H<sub>2</sub>...O<sub>z</sub>) is wider (Fig. 17b), showing a small contribution of O<sub>z</sub> atoms to the displacement of H<sub>2</sub>.

The residence time of the H<sub>2</sub> molecule on the cationic sites is less than 1 ps (~0.22 ps), which is a much shorter duration than for the O<sub>2</sub> molecule (~30 ps). The mobility of the H<sub>2</sub> molecule in the  $\alpha$  cage is therefore more important than that of O<sub>2</sub> although both evolve from a cationic site to another, which is in accordance with the results of Kahn *et al.*<sup>59</sup> who describe the movement of the H<sub>2</sub> molecule in the zeolite as a succession of jumps from one site to another.

**3.2.1. H<sub>2</sub>/H<sub>2</sub>O mixture studies.** Regarding the co-adsorption of H<sub>2</sub> and H<sub>2</sub>O, the observation is the same as for the O<sub>2</sub>/H<sub>2</sub>O mixture, the interaction of the dihydrogen molecule with the cations is not sufficient to remove the H<sub>2</sub>O molecule from its adsorption site whether in the  $\alpha$  or  $\beta$  cage. The only disturb-

ance the H<sub>2</sub> molecule can bring to H<sub>2</sub>O is a reorientation of the latter when the optimised position of the H<sub>2</sub>O molecule is on a pseudostable configuration, which makes it switch to a more stable adsorption site, *e.g.*, the 8R window, as already seen in the H<sub>2</sub>O/O<sub>2</sub> co-adsorption case (Fig. 9d), or when the two molecules interact with the same Na(III) cation (Fig. 18).

In this configuration, the two atoms of H<sub>2</sub> interact with the same Na(III) cation, at H<sub>2</sub>...Na(III) distances of 2.42 and 2.43 Å, while one of them is forming in parallel a hydrogen bond with the oxygen atom of the zeolite (H<sub>2</sub>...O<sub>z</sub> distance of 2.36 Å). The H-H bond length is at 0.76 Å (+0.01 Å compared with the gas phase). However, the oxygen atom of the H<sub>2</sub>O molecule interacts with one Na(I) cation and the Na(III) cation, with which it shares the interaction with H<sub>2</sub>, it also forms a hydrogen bond with the oxygen of the structure, at a H<sub>2</sub>O...O<sub>z</sub> distance of 1.71 Å, which is shorter than the one formed between H<sub>2</sub> and the cage, *i.e.*, the hydrogen bond between the water molecule and the zeolite is stronger than between the dihydrogen molecule and the adsorbant. At the same time, there seems to be no significant interaction between the guest molecules H<sub>2</sub> and H<sub>2</sub>O, and the interaction with the zeolite being favored by both of them.

### 3.3. O<sub>2</sub>/H<sub>2</sub> mixture studies

The absence of an obvious interaction is true between H<sub>2</sub> (or O<sub>2</sub>) and the water molecule, but also between the H<sub>2</sub> and O<sub>2</sub> molecules. Static studies of the simultaneous adsorption of the two molecules inside the Na-LTA zeolite showed that the introduction of a H<sub>2</sub> molecule near the optimised position of the O<sub>2</sub> molecule can disturb its configuration, especially when H<sub>2</sub> is directly placed on the Na<sup>+</sup> cation with which the O<sub>2</sub> molecule is already interacting (Fig. 19).

In this particular configuration, the presence of H<sub>2</sub> causes O<sub>2</sub> to interact with only one Na<sup>+</sup> located on site II, while both atoms of H<sub>2</sub> interact with the same Na(I) with which O<sub>2</sub> has previously interacted. The reasons for this reconfiguration of the O<sub>2</sub> position are, on the one hand, the weakening of the O<sub>2</sub>...Na(I) interaction due to the positioning of H<sub>2</sub> on the same cation, and on the other hand, the distance imposed by the repulsion between O<sub>2</sub> and H<sub>2</sub> that the dynamic calculations

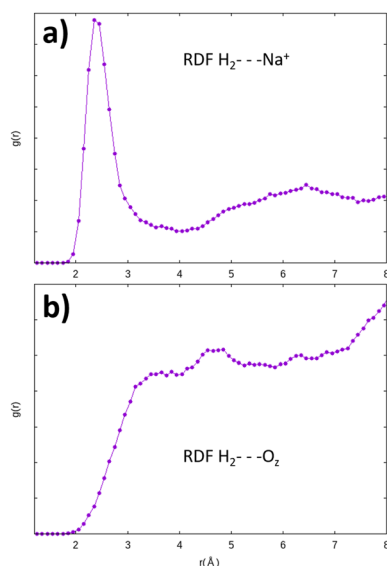


**Fig. 17** Radial distribution function of the H<sub>2</sub>...Na<sup>+</sup> (a) and H<sub>2</sub>...O<sub>z</sub> (b) distances obtained from AIMD calculations – the interaction of H<sub>2</sub> with the Na<sup>+</sup> cation is preponderant.

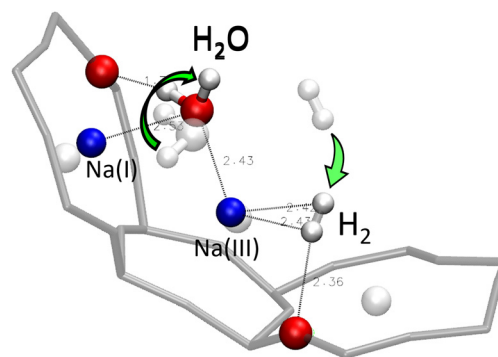


**Fig. 18** Optimised position of the H<sub>2</sub>/H<sub>2</sub>O mixture inside the  $\alpha$  cage after static DFT calculations – the positions of the adsorbed molecules before the optimisation are represented in transparent.



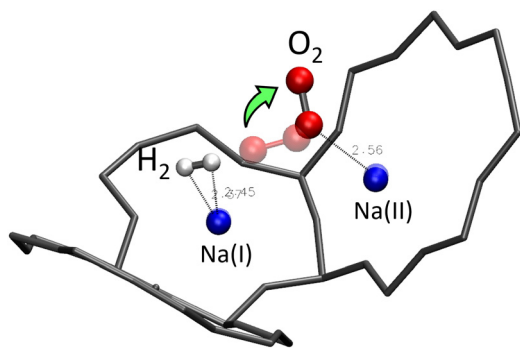


**Fig. 19** Optimised position of the H<sub>2</sub>/O<sub>2</sub> mixture inside the  $\alpha$  cage of the Na-LTA structure after static DFT calculations – the positions of the adsorbed molecules before the optimisation are represented in transparent.

have estimated mainly around 3.85 Å for the co-adsorption of the two molecules inside the  $\alpha$  cage (Fig. 20). Even increasing the probability of meeting between the two molecules by increasing their number in the alpha cage is not enough to sufficiently reduce the O<sub>2</sub>...H<sub>2</sub> distance (which is decreased to 3.35 Å) to form a hydrogen bond.

This value of 3.35 Å is too important to consider the formation of a hydrogen bond between the two molecules even if the probability for this to occur is not zero if we take into account the O<sub>2</sub>...H<sub>2</sub> distances between 2 and 3 Å regarded as weak hydrogen bonds (Fig. 20, 1 O<sub>2</sub> and 1 H<sub>2</sub>). Therefore, as for the O<sub>2</sub> molecule, water is the main regulator of the H<sub>2</sub> molecules access to the cationic sites. Thus, even if the H<sub>2</sub>...Na<sup>+</sup> interaction is weaker than that of O<sub>2</sub>...Na<sup>+</sup>, the impact of the occultation of these cationic sites by water on the H<sub>2</sub> interaction with the zeolite and its mobility should be as consequential as for O<sub>2</sub>. The experimental observation of the consumption of gaseous hydrogen formation, released during water radiolysis in the NaA zeolite,<sup>1</sup> is in line with our numerical calculations. As for O<sub>2</sub> (Fig. 13), the time at which H<sub>2</sub> decays start depends on the water loading rate in the

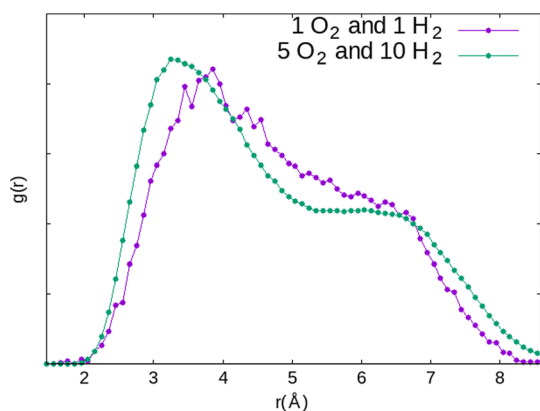


**Fig. 20** Comparison of the RDF of the O<sub>2</sub>...H<sub>2</sub> distance in the  $\alpha$  cage for two systems constituted of different numbers of adsorbates (1O<sub>2</sub> + 1H<sub>2</sub> and 5O<sub>2</sub> + 10H<sub>2</sub>) obtained from AIMD calculations.

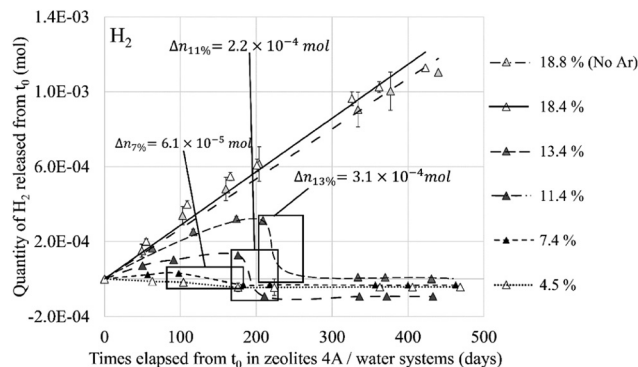


**Fig. 21** Released quantity of H<sub>2</sub> from the NaA zeolite at different water loading rates – framed periods indicate the gas decrease and the quantity of reacting H<sub>2</sub>. Reprinted with permission from L. Frances *et al.*<sup>1</sup> Copyright 2015 American Chemical Society.

zeolite (Fig. 21): the higher the coverage of the Na<sup>+</sup> sites by H<sub>2</sub>O, the later the disappearance of H<sub>2</sub> from the gaseous phase. Also, no decrease was observed when the Na-LTA zeolite is saturated with water, *i.e.*, when no cationic site is available or to interact with H<sub>2</sub>. This behaviour should be observed from the point where all the cationic sites are occupied by H<sub>2</sub>O (at a loading rate of around 13–15%) and eventually O<sub>2</sub>, since the latter has priority over H<sub>2</sub> in their occupation given a stronger O<sub>2</sub> interaction with the cations.

The behaviour of both H<sub>2</sub> and O<sub>2</sub> molecules within the zeolite structure depends on the availability of the cationic sites, which is directly linked to their occupancy by water molecules. Experimental observations of the production and consumption of the two gases<sup>1</sup> highlight this dependence (Fig. 13 and 21). Since a decrease in the quantity was observed for both O<sub>2</sub> and H<sub>2</sub> molecules, the hypothesis of recombination where the zeolite and the water would play a role in the catalyst and inhibitor, respectively, is put forward, considering the application of the Na<sup>+</sup> cations in their adsorption as shown in this work. However, since no direct interaction leading to a reaction between H<sub>2</sub> and O<sub>2</sub> molecules has been noted inside the Na-LTA zeolite, the path to the recombination through the activation of the two molecules *via* the adsorbent surface, as described by L. Benco *et al.*<sup>19</sup> and L. Chen *et al.*<sup>20</sup> is still under study.

## 4. Conclusions

The O<sub>2</sub> molecule exhibits a higher affinity for the Na-LTA zeolite than H<sub>2</sub> despite the fact that both interact with the Na<sup>+</sup> cations. Therefore, as expected, the mobility of the H<sub>2</sub> molecule in the structure is higher compared to that of O<sub>2</sub>, as shown by our *ab initio* molecular dynamics (AIMD) studies. As a result, both molecules evolve from one cationic site to another in the  $\alpha$  cage, but the residence time of the O<sub>2</sub> molecule is significantly longer than that of H<sub>2</sub>. This behaviour around the Na<sup>+</sup> cations leads us to consider that the ‘vectorization’ of the displacement of H<sub>2</sub> increases its probability to meet O<sub>2</sub> while the latter is slowed down on its cationic site,



especially since the studies of the co-adsorption of both molecules have shown that the interaction with the cations is favored rather than with the co-adsorbate. However, inside the hydrated zeolite structure, the cationic sites are mostly occupied by H<sub>2</sub>O molecules and their interaction with the cations is much stronger than those of O<sub>2</sub> and H<sub>2</sub> molecules. Thus, since the water molecule can hardly be removed by H<sub>2</sub> and O<sub>2</sub> from its adsorption site, only the remaining available sites will be occupied by O<sub>2</sub> as shown previously by the RDF calculations (see Fig. 10). An increase of the water loading significantly reduces the possibility of O<sub>2</sub> (and even more for H<sub>2</sub>) to access the Na<sup>+</sup> sites which affect, on the one hand, its mobility and, on the other hand, its activation for the recombination reaction, as described by Acres<sup>9</sup> on the reduction of the reaction rate due to the presence of water on the adsorbant surface. Then, with a high water loading rate, O<sub>2</sub> and H<sub>2</sub> molecules have less interaction with Na<sup>+</sup> cations and higher mobility, thus reducing the probability of encounter between the two *via* a cation-guided trajectory. Experimental studies by L. Frances *et al.*<sup>2</sup> have shown the important role that the amount of water adsorbed in the zeolite has in the production and consumption of O<sub>2</sub> and H<sub>2</sub> (Fig. 13 and 21). Through a simulation study, we have established a link between these experimental observations and the occupancy rate of the cationic sites which states that once all the cationic sites are hydrated, *i.e.*, saturation of the Na<sup>+</sup> sites, the consumption of O<sub>2</sub> and H<sub>2</sub> stops, leading to a continuous production of both gases as can be seen at a water loading rate of ~18% in Fig. 13 and 21. The synchronized disappearance of both O<sub>2</sub> and H<sub>2</sub> being associated with the recombination phenomenon, these combined experimental and simulation results imply that the main actor in the catalytic role of the Na-LTA zeolite for H<sub>2</sub>/O<sub>2</sub> recombination is the Na<sup>+</sup> cation. The availability of cationic sites and the nature of the cation itself are therefore important factors to consider for an efficient catalytic effect of the zeolite.

## Conflicts of interest

There are no conflicts to declare.

## Acknowledgements

The computations in this work were performed on the super-computer facilities of the Mésocentre de calcul de Franche-Comté and on the TGCC (Très Grand Centre de Calcul du CEA). We were granted access to the HPC resources of TGCC under the allocations 2019-A0060910785 and 2020-A0080910785 provided by GENCI.

## References

- 1 L. Frances, M. Douilly, M. Grivet, D. Ducret and M. Théobald, Self-Radiolysis of Tritiated Water Stored in Zeolites 4A: Production and Behavior of H<sub>2</sub> and O<sub>2</sub>, *J. Phys. Chem. C*, 2015, **119**, 28462–28469.
- 2 L. Frances, M. Grivet, J.-P. Renault, J.-E. Groetz and D. Ducret, Hydrogen radiolytic release from zeolite 4A/water systems under  $\gamma$  irradiations, *Radiat. Phys. Chem.*, 2015, **110**, 6–11.
- 3 J. Randrianandraina, M. Badawi, B. Cardey, M. Grivet, J.-E. Groetz, C. Ramseyer, F. T. Anzola, C. Chambelland and D. Ducret, Adsorption of water in Na-LTA zeolites: an ab initio molecular dynamics investigation, *Phys. Chem. Chem. Phys.*, 2021, **23**, 19032–19042.
- 4 S. Motoo and N. Furuya, Hydrogen and oxygen adsorption on Ir (111), (100) and (110) planes, *J. Electroanal. Chem. Interfacial Electrochem.*, 1984, **167**, 309–315.
- 5 J. E. Benson and M. Boudart, Hydrogen-oxygen titration method for the measurement of supported platinum surface areas, *J. Catal.*, 1965, **4**, 704–710.
- 6 J. Clavilier, A. Rodes, K. El Achi and M. Zamakhchari, Electrochemistry at platinum single crystal surfaces in acidic media: hydrogen and oxygen adsorption, *J. Chim. Phys.*, 1991, **88**, 1291–1337.
- 7 A. G. Sault, R. J. Madix and C. T. Campbell, Adsorption of oxygen and hydrogen on Au (110)-(1 $\times$ 2), *Surf. Sci.*, 1986, **169**, 347–356.
- 8 J. L. Gland, G. B. Fisher and E. B. Kollin, The hydrogen-oxygen reaction over the Pt (111) surface: Transient titration of adsorbed oxygen with hydrogen, *J. Catal.*, 1982, **77**, 263–278.
- 9 G. Acres, The reaction between hydrogen and oxygen on platinum, *Platinum Met. Rev.*, 1966, **10**, 60–64.
- 10 L. Morales, *Preliminary report on the recombination rates of hydrogen and oxygen over pure and impure plutonium oxides*, Los Alamos National Laboratory, 1998, pp. 1–37.
- 11 J. A. Lloyd, P. G. Eller and L. Hyder, *Literature search on hydrogen/oxygen recombination and generation in plutonium storage environments*, Los Alamos National Laboratory, LA-UR-98-4557, Los Alamos, NM, 1998.
- 12 K. Chandrakumar and S. Pal, DFT and local reactivity descriptor studies on the nitrogen sorption selectivity from air by sodium and calcium exchanged zeolite-A, *Colloids Surf., A*, 2002, **205**, 127–138.
- 13 P. F. Zito, A. Caravella, A. Brunetti, E. Drioli and G. Barbieri, Light gases saturation loading dependence on temperature in LTA 4A zeolite, *Microporous Mesoporous Mater.*, 2017, **249**, 67–77.
- 14 J. Salazar, S. Lectez, C. Gauvin, M. Macaud, J. Bellat, G. Weber, I. Bezverkhyy and J. Simon, Adsorption of hydrogen isotopes in the zeolite NaX: Experiments and simulations, *Int. J. Hydrogen Energy*, 2017, **42**, 13099–13110.
- 15 N. Bouaziz, M. B. Manaa, F. Aouaini and A. B. Lamine, Investigation of hydrogen adsorption on zeolites A, X and Y using statistical physics formalism, *Mater. Chem. Phys.*, 2019, **225**, 111–121.
- 16 A. Goulay, J. Tsakiris and E. Cohen de Lara, Molecular interactions in nanoporous adsorbents. Adsorption of N<sub>2</sub> and O<sub>2</sub> in zeolites with cavities or channels: Na<sub>2</sub>2A, Ca6A,



- NaX, and decationated mordenite, *Langmuir*, 1996, **12**, 371–378.
- 17 F. Stéphanie-Victoire, A.-M. Goulay and E. Cohen de Lara, Adsorption and coadsorption of molecular hydrogen isotopes in zeolites. 1. Isotherms of H<sub>2</sub>, HD, and D<sub>2</sub> in NaA by thermomicrogravimetry, *Langmuir*, 1998, **14**, 7255–7259.
- 18 J. M. Castillo, J. Silvestre-Albero, F. Rodriguez-Reinoso, T. J. Vlugt and S. Calero, Water adsorption in hydrophilic zeolites: experiment and simulation, *Phys. Chem. Chem. Phys.*, 2013, **15**, 17374–17382.
- 19 L. Benco, T. Bucko, J. Hafner and H. Toulhoat, A density functional theory study of molecular and dissociative adsorption of H<sub>2</sub> on active sites in mordenite, *J. Phys. Chem. B*, 2005, **109**, 22491–22501.
- 20 L. Chen, H. Falsig, T. V. Janssens, J. Jansson, M. Skoglundh and H. Grönbeck, Effect of Al-distribution on oxygen activation over Cu-CHA, *Catal. Sci. Technol.*, 2018, **8**, 2131–2136.
- 21 A. Shubin, G. Zhidomirov, V. Kazansky and R. Van Santen, DFT cluster modeling of molecular and dissociative hydrogen adsorption on Zn<sup>2+</sup> ions with distant placing of aluminum in the framework of high-silica zeolites, *Catal. Lett.*, 2003, **90**, 137–142.
- 22 R. Bell, R. Jackson and C. Catlow, Löwenstein's rule in zeolite A: A computational study, *Zeolites*, 1992, **12**, 870–871.
- 23 W. Loewenstein, The distribution of aluminum in the tetrahedra of silicates and aluminates, *Am. Mineral.*, 1954, **39**, 92–96.
- 24 R. A. Jackson and C. R. A. Catlow, Computer Simulation Studies of Zeolite Structure, *Mol. Simul.*, 1988, **1**, 207–224.
- 25 J. J. Pluth and J. V. Smith, Accurate redetermination of crystal structure of dehydrated zeolite A. Absence of near zero coordination of sodium. Refinement of silicon, aluminum-ordered superstructure, *J. Am. Chem. Soc.*, 1980, **102**, 4704–4708.
- 26 K. Yoshida, K. Toyoura, K. Matsunaga, A. Nakahira, H. Kurata, Y. H. Ikuhara and Y. Sasaki, Atomic sites and stability of Cs<sup>+</sup> captured within zeolitic nanocavities, *Sci. Rep.*, 2013, **3**, 2457.
- 27 G. Kresse and J. Furthmüller, Software VASP, Vienna (1999), *Phys. Rev. B: Condens. Matter Mater. Phys.*, 1996, **54**, 169.
- 28 J. P. Perdew, K. Burke and M. Ernzerhof, Generalized Gradient Approximation Made Simple, *Phys. Rev. Lett.*, 1996, **77**, 3865–3868.
- 29 J. P. Perdew, K. Burke and Y. Wang, Generalized gradient approximation for the exchange-correlation hole of a many-electron system, *Phys. Rev. B: Condens. Matter Mater. Phys.*, 1996, **54**, 16533–16539.
- 30 G. Kresse and D. Joubert, From ultrasoft pseudopotentials to the projector augmented-wave method, *Phys. Rev. B: Condens. Matter Mater. Phys.*, 1999, **59**, 1758–1775.
- 31 P. E. Blöchl, Projector augmented-wave method, *Phys. Rev. B: Condens. Matter Mater. Phys.*, 1994, **50**, 17953–17979.
- 32 S. Grimme, Semiempirical GGA-type density functional constructed with a long-range dispersion correction, *J. Comput. Chem.*, 2006, **27**, 1787–1799.
- 33 T. Bucko, J. Hafner, S. Lebegue and J. G. Angyán, Improved description of the structure of molecular and layered crystals: ab initio DFT calculations with van der Waals corrections, *J. Phys. Chem. A*, 2010, **114**, 11814–11824.
- 34 D. G. Sangiovanni, G. Gueorguiev and A. Kakanakova-Georgieva, Ab initio molecular dynamics of atomic-scale surface reactions: Insights into metal organic chemical vapor deposition of AlN on graphene, *Phys. Chem. Chem. Phys.*, 2018, **20**, 17751–17761.
- 35 C. Liu, H. Gao, A. Hermann, Y. Wang, M. Miao, C. J. Pickard, R. J. Needs, H.-T. Wang, D. Xing and J. Sun, Plastic and superionic helium ammonia compounds under high pressure and high temperature, *Phys. Rev. X*, 2020, **10**, 021007.
- 36 T. Bučko, S. Chibani, J.-F. Paul, L. Cantrel and M. Badawi, Dissociative iodomethane adsorption on Ag-MOR and the formation of AgI clusters: an ab initio molecular dynamics study, *Phys. Chem. Chem. Phys.*, 2017, **19**, 27530–27543.
- 37 Y. Foucaud, S. Lebégue, L. O. Filippov, I. V. Filippova and M. Badawi, Molecular insight into fatty acid adsorption on bare and hydrated (111) fluorite surface, *J. Phys. Chem. B*, 2018, **122**, 12403–12410.
- 38 H. C. Andersen, Molecular dynamics simulations at constant pressure and/or temperature, *J. Chem. Phys.*, 1980, **72**, 2384–2393.
- 39 W. Humphrey, A. Dalke and K. Schulten, VMD: Visual molecular dynamics, *J. Mol. Graphics*, 1996, **14**, 33–38.
- 40 J. D. Gale, GULP: A computer program for the symmetry-adapted simulation of solids, *J. Chem. Soc., Faraday Trans.*, 1997, **93**, 629–637.
- 41 J. Adams, D. Haselden and A. Hewat, The structure of dehydrated Na zeolite A (SiAl = 1.09) by neutron profile refinement, *J. Solid State Chem.*, 1982, **44**, 245–253.
- 42 P. Demontis and G. B. Suffritti, A comment on the flexibility of framework in molecular dynamics simulations of zeolites, *Microporous Mesoporous Mater.*, 2009, **125**, 160–168.
- 43 N. E. Zimmermann, S. Jakobtorweihen, E. Beerdsen, B. Smit and F. J. Keil, In-depth study of the influence of host-framework flexibility on the diffusion of small gas molecules in one-dimensional zeolitic pore systems, *J. Phys. Chem. C*, 2007, **111**, 17370–17381.
- 44 A. García-Sánchez, D. Dubbeldam and S. Calero, Modeling adsorption and self-diffusion of methane in LTA zeolites: the influence of framework flexibility, *J. Phys. Chem. C*, 2010, **114**, 15068–15074.
- 45 D. A. Faux, W. Smith and T. R. Forester, Molecular Dynamics Studies of Hydrated and Dehydrated Na<sup>+</sup>-Zeolite-4A, *J. Phys. Chem. B*, 1997, **101**, 1762–1768.
- 46 T. Chen and T. A. Manz, Bond orders of the diatomic molecules, *RSC Adv.*, 2019, **9**, 17072–17092.
- 47 T. A. Manz, Introducing DDEC6 atomic population analysis: part 3. Comprehensive method to compute bond orders, *RSC Adv.*, 2017, **7**, 45552–45581.
- 48 J. Soussen-Jacob, J. Tsakiris and E. Cohen De Lara, Adsorption of oxygen molecule in NaA zeolite: isotherms



- and infrared measurements, *J. Chem. Phys.*, 1989, **91**, 2649–2655.
- 49 F.-X. Coudert, F. Cailliez, R. Vuilleumier, A. H. Fuchs and A. Boutin, Water nanodroplets confined in zeolite pores, *Faraday Discuss.*, 2009, **141**, 377–398.
- 50 J. Izumi and M. Suzuki, Oxygen selectivity of calcined Na-A type zeolite, *Adsorption*, 2000, **6**, 23–31.
- 51 V. Crupi, D. Majolino, P. Migliardo, V. Venuti and U. Wanderlingh, A FT-IR absorption analysis of vibrational properties of water encaged in NaA zeolites: evidence of a “structure maker” role of zeolitic surface, *Eur. Phys. J. E: Soft Matter Biol. Phys.*, 2003, **12**, 55–58.
- 52 B. Morris, Heats of sorption in the crystalline linde-A zeolite-water vapor system, *J. Colloid Interface Sci.*, 1968, **28**, 149–155.
- 53 A. Baudiquez, Mechanism of recombination of H<sub>2</sub> and O<sub>2</sub> in zeolite : adsorption study on water, M.Sc. thesis, Université de Franche-Comté, 2019.
- 54 M. Falcetta, J. Pazun, M. Dorko, D. Kitchen and P. Siska, Ab initio study of the potential energy surface for the interaction of sodium (1+) with molecular hydrogen and the geometries and energies of Na + (H<sub>2</sub>)<sub>n</sub>, n = 2–4, *J. Phys. Chem.*, 1993, **97**, 1011–1018.
- 55 D. A. Dixon, J. L. Gole and A. Komornicki, Lithium and sodium cation affinities of hydrogen, nitrogen, and carbon monoxide, *J. Phys. Chem.*, 1988, **92**, 1378–1382.
- 56 C. W. Bauschlicher Jr., H. Partridge and S. R. Langhoff, Theoretical study of chromium (1+) and cobalt (1+) bound to hydrogen and nitrogen, *J. Phys. Chem.*, 1992, **96**, 2475–2479.
- 57 C. O. Areán, G. T. Palomino, E. Garrone, D. Nachtigallova and P. Nachtigall, Combined theoretical and FTIR spectroscopic studies on hydrogen adsorption on the zeolites Na-FER and K-FER, *J. Phys. Chem. B*, 2006, **110**, 395–402.
- 58 J. Salazar, M. Badawi, B. Radola, M. Macaud and J. Simon, Quantum effects on the diffusivity of hydrogen isotopes in zeolites, *J. Phys. Chem. C*, 2019, **123**, 23455–23463.
- 59 R. Kahn, E. Cohen de Lara and E. Viennet, Diffusivity of the hydrogen molecule sorbed in NaA zeolite by a neutron scattering experiment, *J. Chem. Phys.*, 1989, **91**, 5097–5102.

